JAMA Neurology | Original Investigation

Kinetics of Human Mutant Tau Prion Formation in the Brains of 2 Transgenic Mouse Lines

Amanda L. Woerman, PhD; Smita Patel, PhD; Sabeen A. Kazmi, BS; Abby Oehler, BS; Yevgeniy Freyman, MS; Lloyd Espiritu, AA; Robert Cotter, BA; Julian A. Castaneda, DVM, PhD; Steven H. Olson, PhD; Stanley B. Prusiner, MD

IMPORTANCE Accumulation of the protein tau is a defining characteristic of several neurodegenerative diseases. Thorough assessment of transgenic (Tg) mouse lines that replicate this process is critical for establishing the models used for testing anti-tau therapeutics in vivo.

OBJECTIVE To define a consistent mouse model of disease for use in future compound efficacy studies.

DESIGN, SETTING, AND PARTICIPANTS In this time course study, cohorts of Tg and control mice were euthanized at defined intervals. Collected brains were bisected down the midline. One half was frozen and used to measure the tau prion content, while the other half was fixed for immunostaining with anti-tau antibodies. All mice were maintained at the Hunters Point Animal Facility at the University of California, San Francisco, and all experiments were performed at the Mission Bay Campus of the University of California, San Francisco. Study animals were PS19, homozygous and hemizygous Tg(MAPT*P301S), and B6/J mice. The study dates were August 9, 2010, to October 3, 2016.

MAIN OUTCOMES AND MEASURES Tau prions were measured using a cell-based assay. Neuropathology was measured by determining the percentage area positive for immunostaining in defined brain regions. A separate cohort of mice was aged until each mouse developed neurological signs as determined by trained animal technicians to assess mortality.

RESULTS A total of 1035 mice were used in this time course study. These included PS19 mice (51.2% [126 of 246] male and 48.8% [120 of 246] female), Tg(MAPT*P301S$^{+/+}$) mice (52.3% [216 of 413] male, 43.8% [181 of 413] female, and 3.9% [16 of 413] undetermined), Tg(MAPT*P301S$^{+/-}$) mice (51.8% [101 of 195] male and 48.2% [94 of 195] female), and B6/J mice (49.7% [90 of 181] male and 50.3% [91 of 181] female). While considerable interanimal variability in neuropathology, disease onset, and tau prion formation in the PS19 mice was observed, all 3 measures of disease were more uniform in the Tg(MAPT*P301S$^{+/+}$) mice. Comparing tau prion formation in Tg(MAPT*P301S$^{+/+}$) mice with B6/J controls, the 95% CIs for the 2 mouse lines diverged before age 5 weeks, and significant ($P < .05$) neuropathology in the hindbrain of 24-week-old mice was quantifiable.

CONCLUSIONS AND RELEVANCE The assessment of disease progression using 3 criteria showed that disease onset in PS19 mice is too variable to obtain reliable measurements for drug discovery research. However, the reproducibility of tau prion formation in young Tg(MAPT*P301S$^{+/+}$) mice establishes a rapid assay for compound efficacy in vivo.

JAMA Neurol. doi:10.1001/jamaneurol.2017.2822
Published online October 23, 2017.

Supplemental content

Author Affiliations: Institute for Neurodegenerative Diseases, Weill Institute for Neurosciences, University of California, San Francisco (Woerman, Patel, Kazmi, Oehler, Freyman, Espiritu, Cotter, Castaneda, Olson, Prusiner); Department of Neurology, University of California, San Francisco (Woerman, Olson, Prusiner); Department of Biochemistry and Biophysics, University of California, San Francisco (Prusiner).

Corresponding Author: Stanley B. Prusiner, MD, Institute for Neurodegenerative Diseases, University of California, San Francisco, Sandler Neurosciences Center, 675 Nelson Rising Ln, San Francisco, CA 94158 (stanley.prusiner@ucsf.edu).

Tau is a soluble protein that stabilizes microtubules in neurons.[1,2] In a group of neurodegenerative diseases termed *tauopathies*, hyperphosphorylated tau accumulates most notably into neurofibrillary tangles (NFTs) in Alzheimer disease (AD).[3] Tauopathies are characterized by progressive dementia,[4] likely resulting from self-propagating misfolded tau (ie, tau prions).[5,6]

After the identification of tau as the main constituent of NFTs in patients with AD,[3,7-9] molecular cloning studies[10,11] found that the tau gene is alternatively spliced into 6 isoforms, giving rise to 0, 1, or 2 N-terminal insertions and 3 or 4 repeats in the repeat domain (RD). The first transgenic (Tg) mouse models expressed 2N4R tau,[12-14] while subsequent models expressed others[15-17] or even all six.[18,19] Discovery of disease-related mutations in tau in 1998 (reviewed by van Swieten and Spillantini[20]) ushered in a new generation of mouse models typically expressing one mutated 4R tau isoform (reviewed by Frank et al[21] and by Dujardin et al[22]). While most patients with tauopathy do not have mutations, the inclusion of mutations, such as P301S, increases the rate of protein misfolding, accelerating disease progression in a mouse model.

To develop therapeutics for patients with tauopathy, Tg mouse models have been characterized based on the animal's ability to recapitulate several features of neurodegeneration, including tau neuropathology, onset of neurological signs, cognitive and motor deficits, and accumulation of tau prions in the brain (reviewed by van Swieten and Spillantini,[20] by Frank et al,[21] and by Dujardin et al[22]). While the currently available models have proven critical for elucidating the molecular pathways underlying disease progression in tauopathies, the lack of comprehensive studies establishing well-defined and reproducible measures of disease progression has hampered the successful discovery of anti-tau therapeutics.

The studies reported herein sought to define consistent measures of disease in a Tg mouse model that could be implemented by drug discovery programs for in vivo compound evaluation. PS19 mice are an often-used model expressing 1N4R tau with the P301S mutation, with tau neuropathology developing by 6 months.[23] However, in our analysis, tau accumulation in almost 8-month-old mice was too inconsistent to provide a meaningful measure of disease. We also found that disease onset in the animals ranged from age 3 to 15 months. Furthermore, despite evidence suggesting that tau prion formation is uniform in PS19 mice,[24,25] we measured 3-fold more tau prions in some animals compared with others tested at the same age.

Given the erratic data collected from PS19 mice, we moved to testing the homozygous Tg(MAPT*P301S$^{+/+}$) mouse model, which expresses 0N4R tau with the P301S mutation.[26] Onset of neurological signs was reported to occur in animals aged 5 to 6 months, suggesting that disease onset in these mice is more synchronized. This is in agreement with our finding herein that only 1.9% (3 of 159) of mice lived beyond 8 months. Moreover, using our group's cell-based assay to measure tau prions,[27] we found that the tau prion content was consistent in young animals, and formation of proteinase K (PK)–resistant tau prions was distinguishable from control animals by 5 weeks. As expected from the reported development of thioflavin S–positive aggregates in Tg(MAPT*P301S$^{+/+}$) mice aged 5 to 6 months,[26] we measured robust tau pathology in 6-month-old mice, but observed a lack of immunostaining in animals aged 4.5 months and younger.

Our results establish a consistent baseline across 3 measures of disease in Tg(MAPT*P301S$^{+/+}$) mice, including neuropathology, disease onset, and tau prion formation. In contrast, we found disease progression in the PS19 mice to be so variable that approximately 900% more animals would be required to adequately power an efficacy study than Tg(MAPT*P301S$^{+/+}$) mice. Moreover, by using a cell-based assay to quantify tau prion formation in the mice, we identified an early end point for efficacy studies that directly measures biologically active tau.

Key Points

Question What is a reproducible baseline measure of disease progression in a tauopathy animal model that we can use to determine compound efficacy in drug discovery programs?

Findings A total of 1035 mice were used in this time course study. In 1 line of transgenic mice, tau prions were reproducibly detected by age 5 weeks, while extensive variability in another mouse line renders the model unusable for efficacy studies.

Meaning Future studies assessing the ability of small molecules or other therapeutic strategies to slow or halt neurodegeneration should directly measure the ability of the compound to halt tau prion formation in an animal model that exhibits consistent disease kinetics.

Methods

Study Design

In this time course study, cohorts of Tg and control mice were euthanized at defined intervals. Collected brains were bisected sagittally. One half was frozen and used to measure the tau prion content, while the other half was fixed for immunostaining with anti-tau antibodies. All animals were maintained at the Hunters Point Animal Facility at the University of California, San Francisco, and all experiments were performed at the Mission Bay Campus of the University of California, San Francisco. Study animals were PS19, homozygous and hemizygous Tg(MAPT*P301S), and B6/J mice. The study dates were August 9, 2010, to October 3, 2016.

Animals were maintained in a facility accredited by the Association for Assessment and Accreditation of Laboratory Animal Care in accord with the *Guide for the Care and Use of Laboratory Animals*.[28] All procedures were approved by the University of California, San Francisco, Institutional Animal Care and Use Committee. Animals were maintained under standard environmental conditions, with a cycle of 12 hours' light and 12 hours' dark and free access to food and water. Animals used in this study include C57BL/6J (B6/J) mice[29] (Jackson Laboratory; https://www.jax.org/strain/000664), PS19 mice,[23] and homozygous and hemizygous B6-Tg(Thy1-MAPT*P301S)2541 mice.[26]

Tau prions were measured using a cell-based assay. Neuropathology was measured by determining the percentage area

positive for immunostaining in defined brain regions. A separate cohort of mice was aged until each mouse developed neurological signs as determined by trained animal technicians to assess mortality.

Tau Prion Assay

A 10% brain homogenate was prepared using frozen half-brains from B6/J and Tg(MAPT*P301S) mice in calcium and magnesium-free 1 × Dulbecco phosphate-buffered saline (DPBS) (Thermo Fisher). Protein aggregates were precipitated using sodium phosphotungstic acid (Sigma), as described previously.[30,31] Protein pellets were diluted 1:4 in 1 × DPBS and tested in the cell aggregation assay.

Culture and assay conditions for human embryonic kidney (HEK293) cells expressing Tau(4RD*LM)-YFP(1)[32] were previously described, where LM indicates the 2 familial mutations P301L and V337M and YFP indicates yellow fluorescent protein.[27] After 4 days' incubation, 384-well plates were imaged using the IN Cell Analyzer 6000 (GE Healthcare Life Sciences). 4′,6-Diamidino-2-phenylindole and fluorescein isothiocyanate images were collected from 4 regions in each well, which were analyzed using the IN Cell Developer software. Each sample was tested independently 3 times.

Additional eMaterials and eMethods are available in the eAppendix in the Supplement. The significance level in the study was set at 2-sided $P < .05$ for statistical analyses performed with a *t* test.

Results

A total of 1035 mice were used in this time course study. These included PS19 mice (51.2% [126 of 246] male and 48.8% [120 of 246] female), Tg(MAPT*P301S$^{+/+}$) mice (52.3% [216 of 413] male, 43.8% [181 of 413] female, and 3.9% [16 of 413] undetermined), Tg(MAPT*P301S$^{+/-}$) mice (51.8% [101 of 195] male and 48.2% [94 of 195] female), and B6/J mice (49.7% [90 of 181] male and 50.3% [91 of 181] female).

Variability of Tauopathy Progression in PS19 Mice

Two-month-old PS19 mice[23] were inoculated intracranially with 30 µL of either 1 × DPBS or 1% control brain homogenate diluted in 5% bovine serum albumin. The mice were collected at age 31 weeks, and the formalin-fixed brains were assessed for tau neuropathology using the antibody AT8 (phosphorylated tau at Ser202/Thr205) (eFigure 1A in the Supplement). Studies of central nervous system disease proved infeasible due to random variations in tau neuropathology. In a separate group of mice used to assess disease onset, shown in a Kaplan-Meier plot (red line in eFigure 1B in the Supplement), neurological signs required 3 to 15 months to develop. When we performed our initial PS19 mouse survival studies, we were unaware of the variation in the published mortality data (black line in eFigure 1B in the Supplement).[23]

To determine the tau prion content of the brains from PS19 mice, we collected frozen half-brains from mice aged 20 to 38 weeks and measured the tau prion levels using a cell-based assay.[31] Clarified brain homogenate was incubated with HEK293T cells expressing the RD of 4R tau containing the P301L and V337M mutations fused to YFP [Tau(4RD*LM)-YFP(2) cells] for 3 days (eFigure 1C and D in the Supplement). These cells formed aggregates in the presence of tau prions but not when incubated with control samples.[31] Tau prion infection was measured using the sum of total fluorescence from all aggregates divided by cell count (density × area [D × A] per cell ×10^3 arbitrary units [AU]) and the percentage of cells containing aggregates. Consistent with the neuropathology and mortality data, the rate of tau prion formation in the PS19 mice was variable, with some 38-week-old mice having 3-fold more tau prions than others.

Tau Prion Formation in Tg(MAPT*P301S$^{+/+}$) Mice

Using the Tg(MAPT*P301S$^{+/+}$) line,[26] we compared spontaneous tau prion formation in frozen half-brains with wild-type B6/J mice in the cell-based assay.[27] Tau prions from brains of mice aged 2 to 30 weeks were isolated from 10% brain homogenates by phosphotungstic acid precipitation,[30] and the prions were assayed using Tau(4RD*LM)-YFP(1) cells (**Figure 1** and eFigure 2 and eFigure 3 in the Supplement). Wild-type B6/J mouse samples did not infect Tau(4RD*LM)-YFP(1) cells (eFigure 2C and eFigure 3A in the Supplement); however, Tg(MAPT*P301S$^{+/+}$) samples infected cells with an approximately linear increase in prion formation (Figure 1A and eFigure 3B in the Supplement).

To determine the age at which Tg(MAPT*P301S$^{+/+}$) mice became distinguishable from B6/J mice, nonparametric curves were fit to the data, and the 95% CI was calculated. Significant separation between the 2 lines was defined as the age at which the 95% CIs no longer overlapped. Tg(MAPT*P301S$^{+/+}$) mice were significantly different from B6/J mice at age 4.4 weeks using D × A per cell (Figure 1B and C) and at age 3.1 weeks using percentage of cells with aggregates (eFigure 3C and D in the Supplement). These analyses demonstrate that spontaneous tau prion formation was quantifiable by age 3 to 5 weeks in Tg(MAPT*P301S$^{+/+}$) mice.

Tau Prion Formation More Uniform in Young Tg(MAPT*P301S$^{+/+}$) Mice

Assessing possible differences in tau prion formation between male and female Tg(MAPT*P301S$^{+/+}$) mice, we plotted D × A per cell measurements from each animal by sex (**Figure 2**A). Through 12 weeks, both male and female mice showed a linear increase in tau prion formation (Figure 2B), suggesting that assays measuring the reduction in tau prion propagation in young Tg(MAPT*P301S$^{+/+}$) mice might facilitate anti-tau drug discovery. The tau prion content in older animals was more variable than in younger mice.

Neurological Dysfunction in Tg(MAPT*P301S$^{+/+}$) Mice

Onset of neurological signs was observed in a separate group of Tg(MAPT*P301S$^{+/+}$) mice at approximately age 24 weeks (Figure 2C). Females developed degenerative signs before males. The high variability in tau prions measured in the cell assay at the 20-week time point coincides with onset of neurological signs. Comparison of Kaplan-Meier plots from Tg(MAPT*P301S$^{+/+}$) and PS19 mice reveal that Tg(MAPT*P301S$^{+/+}$) mice exhibit a more uniform disease onset (eFigure 1B in the Supplement). To compare

Figure 1. Spontaneous Tau Prion Formation Occurs Before Age 5 Weeks in Tg(MAPT*P301S$^{+/+}$) Mice

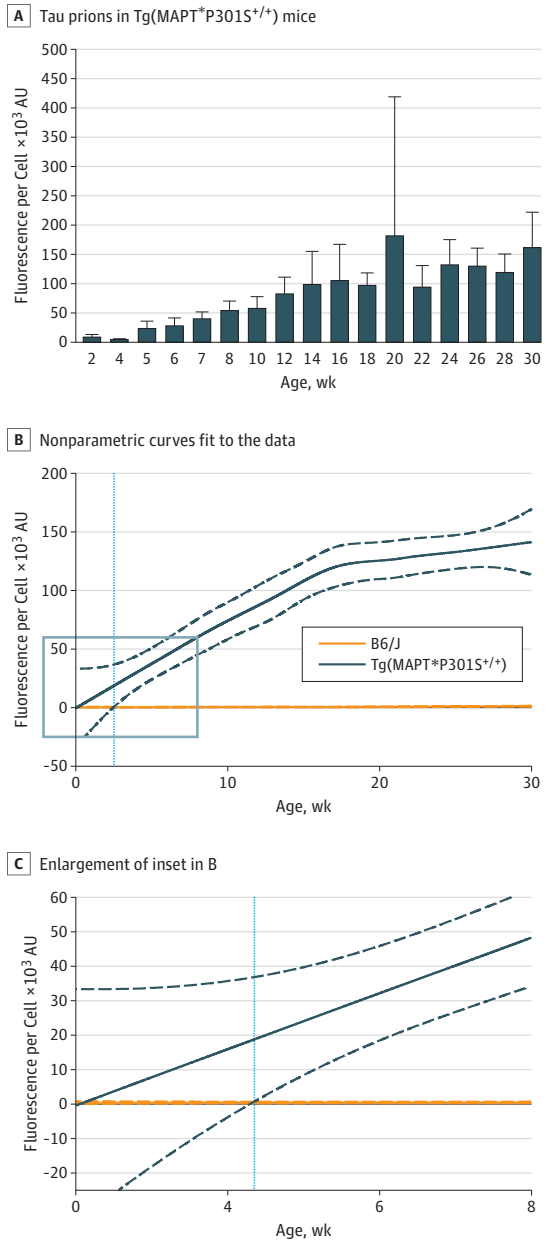

Tau prions were isolated from B6/J and Tg(MAPT*P301S$^{+/+}$) mouse brain homogenates using sodium phosphotungstic acid. Protein pellets were diluted 1:4 in 1 × Dulbecco phosphate-buffered saline and incubated with Tau(4RD*LM)-YFP(1) cells for 4 days before imaging. A, After incubating with protein isolated from Tg(MAPT*P301S$^{+/+}$) mice, infected cells were quantified by dividing the total fluorescence in each image by the number of living cells (×10^3 arbitrary units [AU]). The time course of spontaneous tau prion formation was quantified by testing samples from mice aged 2 to 30 weeks. Data are shown as the mean (SD) for each time point. B, Nonparametric curves were fit to the data collected from each B6/J mouse (solid orange line) and each Tg(MAPT*P301S$^{+/+}$) mouse (solid dark blue line). The 95% CI was calculated for both mouse lines (dotted lines), and the age at which the 2 95% CIs no longer overlapped (age 4.4 weeks) was determined (light blue line). C, The inset (gray box) in B is enlarged in C.

this difference statistically, a power analysis was performed to determine the sample size needed to adequately power efficacy studies using both lines (eTable in the Supplement). Regardless of expected effect size, at least 900% more PS19 than Tg(MAPT*P301S$^{+/+}$) mice would be required to adequately power an efficacy study. An effect size of 10%, which is necessary for establishing a dose response or selecting a clinical candidate, would require a total of 8 Tg(MAPT*P301S$^{+/+}$) or 92 PS19 mice. However, because the hemizygous PS19 mice are bred with noncarriers, breeding at least 184 mice would be required to carry out one efficacy study.

Neuropathological Lesions in Tg(MAPT*P301S$^{+/+}$) Mice

The kinetics of tau neuropathology in Tg(MAPT*P301S$^{+/+}$) mice were analyzed in formalin-fixed half-brains from Tg(MAPT*P301S$^{+/+}$) and B6/J mice aged 6, 12, 18, and 24 weeks, by immunostaining with AT8, MC1 (misfolded tau), HT7 (human tau), and glial fibrillary acidic protein (GFAP) antibodies. The sensorimotor cortex, striatum, piriform cortex and amygdala, hippocampus, thalamus, hypothalamus, midbrain, and pons were evaluated in all animals.

No AT8 neuropathology was found in B6/J mice (**Figure 3** and eFigure 4 in the Supplement). Comparing AT8 deposition between 6-week-old B6/J and Tg(MAPT*P301S$^{+/+}$) mice, a small but significant increase in the midbrain and pons was found. A much larger increase in AT8 staining was observed in the brains of Tg(MAPT*P301S$^{+/+}$) mice at age 24 weeks compared with 6-week-old animals as well as compared with 24-week-old B6/J mice. The MC1 and HT7 immunostaining yielded similar results, with significant detection of tau aggregates in 24-week-old Tg(MAPT*P301S$^{+/+}$) mice but minimal immunostaining in younger animals (eFigure 4 and eFigure 5 in the Supplement).

In parallel, measuring astrogliosis with the GFAP antibody (eFigure 6 in the Supplement) showed that reactive astrocytes were significantly increased in the thalamus, midbrain, and pons of 24-week-old Tg(MAPT*P301S$^{+/+}$) mice compared with 6-week-old Tg(MAPT*P301S$^{+/+}$) animals. As expected, GFAP immunostaining was unchanged through age 24 weeks in the B6/J mice.

Stability of Tau Prions From Tg(MAPT*P301S$^{+/+}$) Mice

Given the neuropathological differences between 6-week-old and 24-week-old Tg(MAPT*P301S$^{+/+}$) mice, we examined tau prion stability from animals aged 6 weeks and 24 weeks under denaturing conditions (**Figure 4**). Tau prions from aged Tg(MAPT*P301S$^{+/+}$) mice were previously found to be resistant to 1 µg/mL of PK.[33] Testing tau prions from two 6-week-old and 24-week-old Tg(MAPT*P301S$^{+/+}$) mice, 1 mg of detergent-insoluble protein was digested in 0, 0.5, 1, 2.5, or 5 µg of PK for 30 minutes (Figure 4A and B). The remaining protein was analyzed by immunoblot using the human tau antibody Tau12. Tau prions from both the 6-week-old and 24-week-old mice were resistant to 1 µg of PK, were partially digested by 2.5 µg of PK, and were completely digested by 5 µg of PK.

We also tested stability by sequential extraction in detergents with an increasing propensity to solubilize aggregated protein (Figure 4C). This method identified differences in

Figure 2. Spontaneous Tau Prion Formation Is Not Affected by Sex Differences in Young Tg(MAPT*P301S$^{+/+}$) Mice

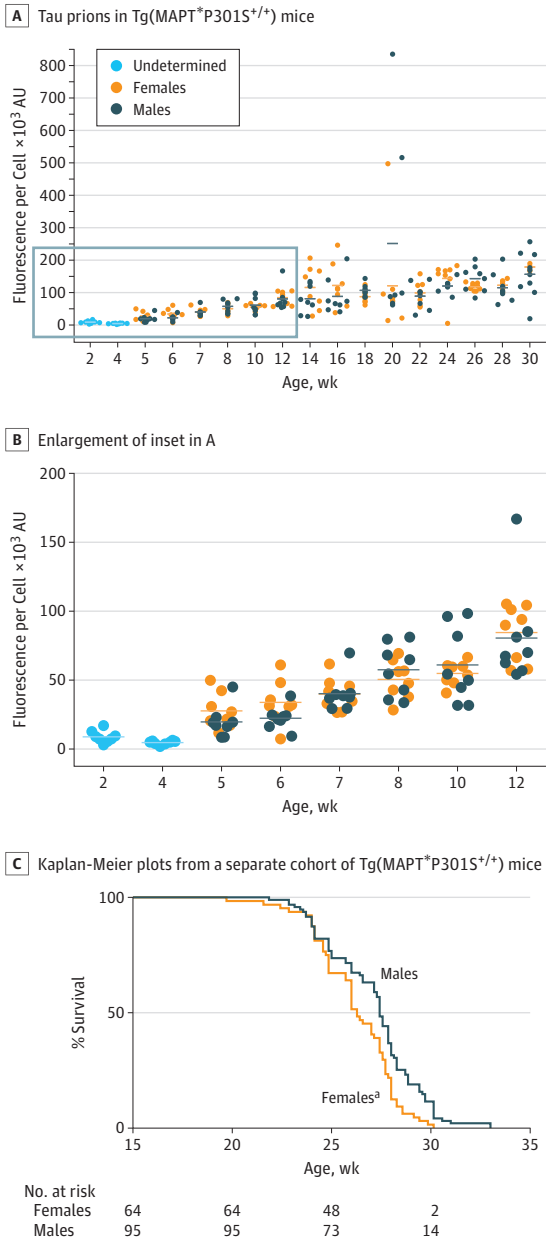

A and B, Individual fluorescence per cell measurements (×10^3 arbitrary units [AU]) collected from Tau(4RD*LM)-YFP(1) cells after incubation with protein aggregates isolated from Tg(MAPT*P301S$^{+/+}$) mice were plotted by sex. The inset (gray box) in A is enlarged in B. Each dot represents the average of 3 independent preparations tested from each mouse. C, Kaplan-Meier plots from a separate cohort of animals show that disease onset in female Tg(MAPT*P301S$^{+/+}$) mice (orange) occurs before that in males (dark blue). [a]P = .002.

Figure 3. AT8 Neuropathology in Tg(MAPT*P301S$^{+/+}$) Mice Increases at Age 24 Weeks

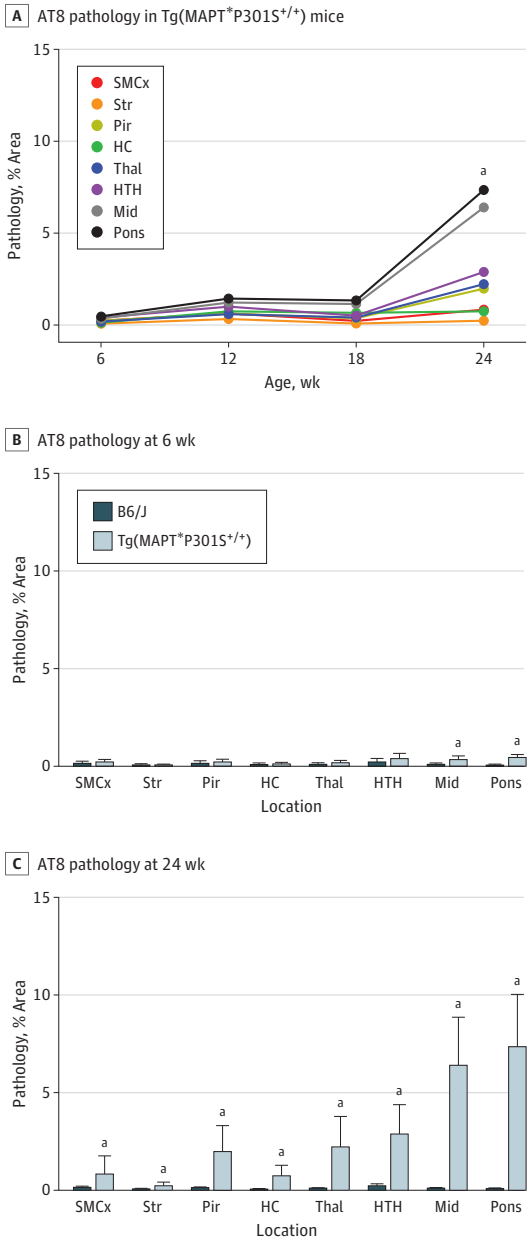

AT8 neuropathology was measured in the sensorimotor cortex (SMCx), striatum (Str), piriform cortex and amygdala (Pir), hippocampus (HC), thalamus (Thal), hypothalamus (HTH), midbrain (Mid), and pons of B6/J and Tg(MAPT*P301S$^{+/+}$) mice aged 6, 12, 18, and 24 weeks. A, Time course of AT8 neuropathology in Tg(MAPT*P301S$^{+/+}$) mice. AT8 neuropathology was significantly increased in all brain regions in Tg(MAPT*P301S$^{+/+}$) mice at age 24 weeks compared with mice at age 6 weeks (P = .02 for SMCx, P = .004 for Str, P < .001 for Pir, P < .001 for HC, P < .001 for Thal, P < .001 for HTH, P < .001 for Mid, and P < .001 for pons). Data are given as the means. B and C, Comparing AT8 neuropathology by brain region in B6/J and Tg(MAPT*P301S$^{+/+}$) mice. AT8 pathology was increased in the Mid (P = .02) and pons (P < .001) of 6-week-old Tg(MAPT*P301S$^{+/+}$) mice (B) compared with B6/J mice (C) and was increased in all brain regions in 24-week-old animals (P = .01 for SMCx, P = .003 for Str, P < .001 for Pir, P < .001 for HC, P < .001 for Thal, P < .001 for HTH, P < .001 for Mid, and P < .001 for pons). Data are shown as the mean (SD). [a]P < .05.

protein solubility in several Tg mouse models.[23,34-36] Brain homogenates were digested in high salt, high salt plus Triton X-100, radioimmunoprecipitation buffer, 2% sodium dodecylsulfate, and 66% formic acid; the supernatant from each extraction was collected for immunoblot analysis, while the protein pellet was digested in the subsequent buffer. Tau prions

Figure 4. Spontaneous Tau Prions Isolated From Tg(MAPT*P301S$^{+/+}$) Mouse Brains Are Stable Under Denaturing Conditions

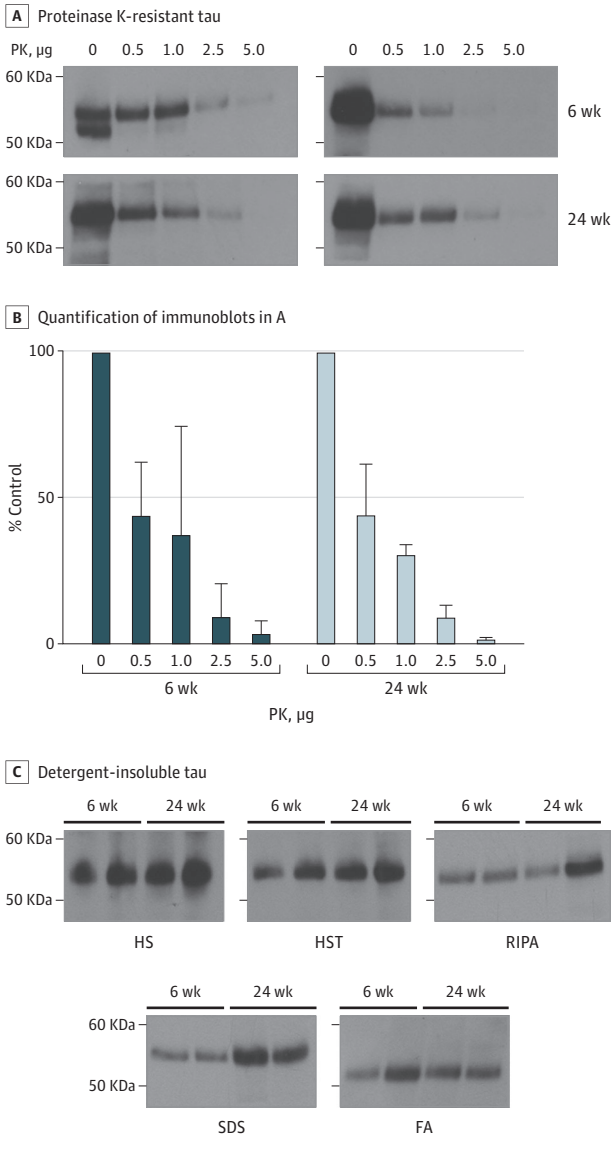

A, Detergent-insoluble protein (1 mg) was isolated from male Tg(MAPT*P301S$^{+/+}$) mice at age 6 weeks and 24 weeks (n = 2) and digested with increasing concentrations of proteinase K (PK) (0-5 µg) at 37°C for 30 minutes (while shaking). Protein remaining after partial digestion was pelleted by ultracentrifugation and analyzed by Western blot with the Tau12 antibody. B, Quantification of immunoblots shown in A were normalized to 0 µg of PK. Data are shown as the mean (SD) for the 2 mice at each time point. C, Aggregated protein was isolated from 6-week-old and 24-week-old male Tg(MAPT*P301S$^{+/+}$) mice (n = 2) using a series of increasingly stringent buffers, including high salt (HS), high salt plus Triton X-100 (HST), radioimmunoprecipitation buffer (RIPA), 2% sodium dodecylsulfate (SDS), and 66% formic acid (FA). Soluble fractions were collected after digestion in each buffer and were analyzed by Western blot with the Tau12 antibody.

from 6-week-old and 24-week-old mice demonstrated similar resistance in all 5 detergents. Together, these stability data argue that tau prions in 6-week-old and 24-week-old Tg(MAPT*P301S$^{+/+}$) mice are similar.

Tau Prion Formation Kinetics Modified by Transgene Dose

To determine the influence of transgene dose on tau prion formation, we collected frozen half-brains from 6-week-old to 24-week-old hemizygous Tg(MAPT*P301S$^{+/-}$) mice (**Figure 5**A and B and eFigure 7A in the Supplement). Incubating tau prions isolated from Tg(MAPT*P301S$^{+/-}$) mice with Tau(4RD*LM)-YFP (1) cells showed an increase in tau prion formation with age. After calculating the 95% CI for these data, we determined that Tg(MAPT*P301S$^{+/-}$) mice can be distinguished from B6/J mice at age 7.9 weeks using D × A per cell (black line in Figure 5B and eFigure 7B in the Supplement) and at age 7.3 weeks using percentage cells with aggregates (blue line in eFigure 8B and C in the Supplement). Homozygous Tg(MAPT*P301S$^{+/+}$) mice were significantly different from hemizygous animals before age 6 weeks (gray line in Figure 5B and green line in eFigure 8 in the Supplement). The concentration of tau prions in aged Tg(MAPT*P301S$^{+/-}$) mouse brains remained below the concentration in 12-week-old homozygous mice.

We also examined tau and GFAP neuropathology in Tg(MAPT*P301S$^{+/-}$) mice aged 6, 12, 18, and 24 weeks. AT8 neuropathology was similar in 6-week-old B6/J and Tg(MAPT*P301S$^{+/-}$) mice (eFigure 9 in the Supplement) and in 6-week-old and 24-week-old Tg(MAPT*P301S$^{+/-}$) mice (eFigure 10A and B in the Supplement). Significant, although minute, increases in AT8 immunostaining were quantified in the midbrain and pons of 24-week-old Tg(MAPT*P301S$^{+/-}$) mice relative to B6/J mice (eFigure 9 in the Supplement). In comparison, tau neuropathology in 24-week-old Tg(MAPT*P301S$^{+/-}$) mice was significantly reduced compared with 24-week-old homozygous mice (Figure 5C).

Tau immunostaining using the MC1 and HT7 antibodies showed similar results as obtained with the AT8 antibody (eFigure 10C-F in the Supplement). In addition, no differences in astrogliosis were observed between 6-week-old and 24-week-old Tg(MAPT*P301S$^{+/-}$) mice with the exception of a small decrease in the midbrain (eFigure 11 in the Supplement). Consistent with the tau prion quantification assay, we observed remarkably less neuropathology in 24-week-old hemizygous mice compared with homozygous mice.

Finally, we compared the spontaneous onset of neurological signs in a separate cohort of animals (green line in eFigure 1B in the Supplement). While Tg(MAPT*P301S$^{+/-}$) mice exhibited a similar rate of disease onset as observed in PS19 mice, approximately 40% fewer animals would be required to adequately power an efficacy study using this line (eTable in the Supplement). However, compared with the homozygous mice, almost 600% more Tg(MAPT*P301S$^{+/-}$) animals would be required.

Discussion

Transgenic animal models have contributed greatly to elucidating the molecular mechanisms that feature in neurodegenerative disorders. For tauopathies, mouse models replicating neuropathological lesions seen in human patients have resulted in important discoveries regarding the spreading of misfolded tau throughout the brain. However, to focus efforts on discovering drugs that intervene with tau prion replication,

reproducible animal models of tau prion propagation must be generated. Toward that end, our studies demonstrate that Tg(MAPT*P301S$^{+/+}$) mice, but not PS19 mice, accumulate reproducible levels of tau prions in Tg mouse brain. The early accumulation of measurable levels of tau prions makes Tg(MAPT*P301S$^{+/+}$) mice more suitable for drug discovery studies.

In a recent PubMed search, among the 330 publications currently citing the study by Yoshiyama et al[23] that first reported the PS19 mouse line, we found that 60 reports had used the mice for primary research studies, including the original publication. Given the frequent use of the PS19 model in at least 17 studies[23,37-52] containing efficacy data, we sought to measure disease progression in this mouse line. AT8 immunostaining in 31-week-old PS19 mice revealed substantial interanimal variability, rendering neuropathology an unreliable end point for evaluating future efficacy studies. Subsequent analysis of onset of neurological dysfunction also identified extensive variability in the PS19 mice. Likewise, quantification of tau prion formation in 22-week-old to 38-week-old animals using the Tau(4RD*LM)-YFP(2) cell assay[31] found that the rate of formation often resulted in a 3-fold difference in the tau prion content within a cohort of animals. Our findings contradict several previous reports showing consistent tau prion formation over time in 4 different brain regions in the mice.[24,25] This difference may arise from not microdissecting brain regions prior to infecting cells. Additionally, we use an equal distribution of males and females herein, but it has been reported that PS19 males develop pathology more consistently than females.[38]

In contrast with the PS19 mice, tau prions were quantifiable in 5-week-old Tg(MAPT*P301S$^{+/+}$) mice, and the rate of tau prion formation in young Tg(MAPT*P301S$^{+/+}$) mice consistently increased regardless of sex. While neuropathological changes were reproducible in Tg(MAPT*P301S$^{+/+}$) mice, significant lesions were only found in the 24-week-old mice. Given this stark difference between the neuropathological changes in 6-week-old and 24-week-old Tg(MAPT*P301S$^{+/+}$) mice, the biochemical properties of tau prions isolated from Tg(MAPT*P301S$^{+/+}$) mice at both ages were compared, and similar resistance to several protein-denaturing conditions was observed, irrespective of animal age. These similar properties suggest that in vivo assays measuring the influence of drug candidates on the tau prion content in young mice are feasible. Using young Tg(MAPT*P301S$^{+/+}$) mice instead of older animals (or PS19 mice) should permit a more rapid measurement of tau prions in the brains of treated animals.

There are 3 likely sources contributing to the identified differences between these 2 models. First, the Tg(MAPT*P301S$^{+/+}$) mice are on a congenic B6/J background, but the PS19 mice are on a hybrid B6C3 background. The PS19 mice are available on a congenic B6/J background from The Jackson Laboratory, but the line is not actively bred. More important, because the PS19 mice are most commonly used on the B6C3 background, we chose to perform our studies using that version of the model. The variability of disease onset conferred by a mixed-strain background has been well documented in scrapie transmission studies,[53-57] suggesting that it may have a role in tauopathy progression as well. Second, the promoter used to drive

Figure 5. Disease Onset Is Delayed in Tg(MAPT*P301S$^{+/-}$) Mice

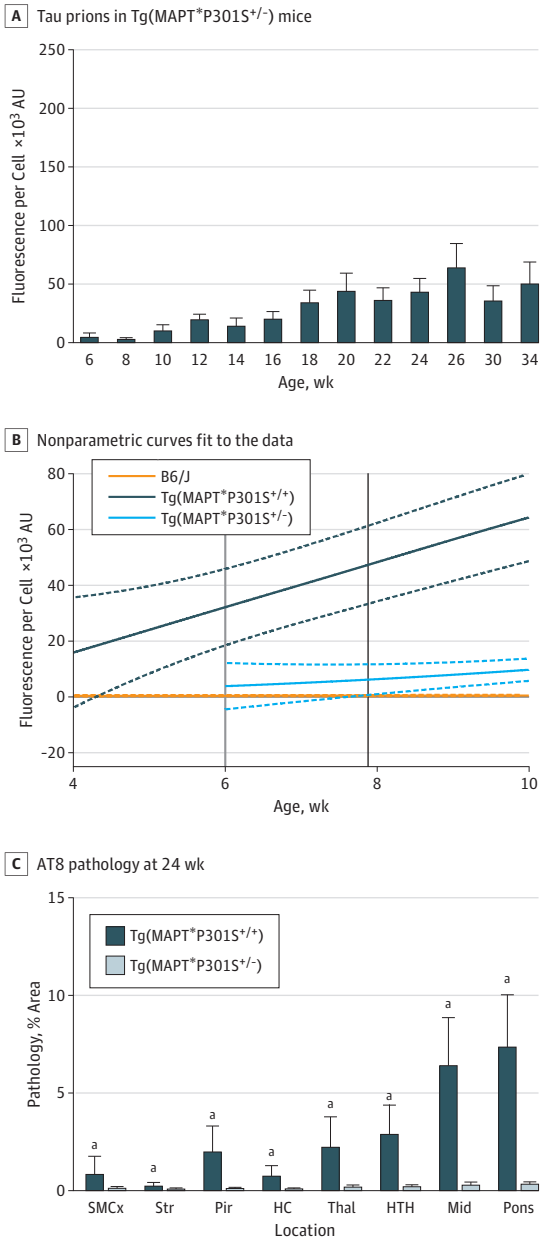

A, Tau prions isolated from 6- to 34-week-old Tg(MAPT*P301S$^{+/-}$) mice were diluted 1:4 in 1 × Dulbecco phosphate-buffered saline and incubated with Tau(4RD*LM)-YFP (1) cells for 4 days. The mean (SD) of tau prion infection in Tau(RD*LM)-YFP(1) cells was measured by total fluorescence per cell (×10^3 arbitrary units [AU]). Tau prions were quantified from each animal by averaging 3 independent preparations. B, A nonparametric curve was fit to the data in A (solid light blue line). The 95% CI was calculated (dotted lines) and compared with curves generated from the B6/J (orange line) and Tg(MAPT*P301S$^{+/+}$) (dark blue lines) data. The age at which the 95% CIs for the Tg(MAPT*P301S$^{+/-}$) and Tg(MAPT*P301S$^{+/+}$) mice no longer overlapped occurred before 6 weeks (gray line). The separation in 95% CIs with the B6/J mice occurred at 7.9 weeks (black line). C, AT8 neuropathology measured in the sensorimotor cortex (SMCx), striatum (Str), piriform cortex and amygdala (Pir), hippocampus (HC), thalamus (Thal), hypothalamus (HTH), midbrain (Mid), and pons of 24-week-old Tg(MAPT*P301S$^{+/-}$) mice was reduced in all brain regions compared with Tg(MAPT*P301S$^{+/+}$) mice (P = .008 for SMCx, P = .008 for Str, P < .001 for Pir, P < .001 for HC, P < .001 for Thal, P < .001 for HTH, P < .001 for Mid, and P < .001 for pons). Data are given as the mean (SD).
[a] P < .05.

transgene expression differs between the lines; the Tg(MAPT*P301S$^{+/+}$) mice rely on the *Thy1* promoter, while the PS19 mice use the *Prnp* promoter. Both are neuron specific but differ in location and level of expression.[58-61] Neuropathology in these mice manifests with differing spatial distributions, indicating that the promoter influences disease progression.[23,26] Third, transgene dose differs between the 2 models; support for a dose effect is provided by the delayed disease onset in Tg(MAPT*P301S$^{+/-}$) mice compared with the homozygous animals. Moreover, the Tg(MAPT*P301S$^{+/-}$) Kaplan-Meier plot shows variable disease onset that is comparable with the PS19 mice. Female homozygous PS19 mice do not breed, making it unfeasible to establish a homozygous colony.

Limitations

As Tg models of neurodegeneration that develop spontaneous tau prions, it is unclear if the PS19 and Tg(MAPT*P301S) mouse models develop tau prion strains that are consistent with the tau prion strains present in humans with tauopathy. Moreover, the lack of therapeutics with demonstrated success in clinical trials limits our ability to evaluate the sensitivity of this efficacy model against control compounds.

Conclusions

The results reported herein have important implications for the ongoing efforts to discover anti-tau therapeutics and illustrate the need for uniform disease progression in efficacy models. In establishing the kinetics of tau prion replication in Tg(MAPT*P301S$^{+/+}$) mice, we demonstrate that formation and propagation of tau prions precede the development of neuropathological lesions in the brain and, as a result, represent a reproducible end point for evaluating compound efficacy in Tg(MAPT*P301S$^{+/+}$) mice.

ARTICLE INFORMATION

Accepted for Publication: July 23, 2017.

Published Online: October 23, 2017. doi:10.1001/jamaneurol.2017.2822

Author Contributions: Dr Woerman had full access to all of the data in the study and takes responsibility for the integrity of the data and the accuracy of the data analysis.
Study concept and design: Woerman, Castaneda, Olson, Prusiner.
Acquisition, analysis, or interpretation of data: All authors.
Drafting of the manuscript: Woerman, Olson.
Critical revision of the manuscript for important intellectual content: All authors.
Statistical analysis: Woerman.
Obtained funding: Prusiner.
Administrative, technical, or material support: Woerman, Patel, Kazmi, Oehler, Freyman, Espiritu, Cotter, Castaneda.
Study supervision: Woerman, Olson, Prusiner.

Conflict of Interest Disclosures: Dr Prusiner reported being the chair of the scientific advisory board of Alzheon, Inc, which has not contributed financial or any other support to the studies herein. No other disclosures were reported. The Institute for Neurodegenerative Diseases has a research collaboration with Daiichi Sankyo (Tokyo, Japan).

Funding/Support: This work was supported by grants AG002132 and AG031220 from the National Institutes of Health, as well as by support from The Henry M. Jackson Foundation for the Advancement of Military Medicine, the Rainwater Charitable Foundation, the Glenn Foundation for Medical Research, the Mary Jane Brinton Fund, and Daiichi Sankyo (all to Dr Prusiner).

Role of the Funder/Sponsor: The funding sources had no role in the design and conduct of the study; collection, management, analysis, and interpretation of the data; preparation or review of the manuscript; and decision to submit the manuscript for publication. Daiichi Sankyo approved the manuscript.

Additional Contributions: Michel Goedert, PhD, at the Division of Neurobiology, Cambridge Neuroscience, University of Cambridge, Cambridge, England, provided the Tg(MAPT*P301S)$^{+/+}$ mice, and the Hunters Point Animal Facility staff at the University of California, San Francisco, bred and cared for the animals used in this study. At the Institute for Neurodegenerative Diseases, University of California, San Francisco, Jeffrey Lau, BS, and Rigoberto Roman-Albarran, BS, assisted with processing mouse samples, and George A. Carlson, PhD, contributed thoughtful input and revisions to the manuscript. None received compensation.

REFERENCES

1. Cleveland DW, Hwo SY, Kirschner MW. Purification of tau, a microtubule-associated protein that induces assembly of microtubules from purified tubulin. *J Mol Biol*. 1977;116(2):207-225.

2. Iqbal K, Grundke-Iqbal I, Zaidi T, et al. Defective brain microtubule assembly in Alzheimer's disease. *Lancet*. 1986;2(8504):421-426.

3. Brion JP, Passareiro H, Nunez J, Flament-Durand J. Immunological determinants of tau proteins are present in neurofibrillary tangles of Alzheimer's disease [in French]. *Arch Biol (Liege)*. 1985;95:229-235.

4. Williams DR. Tauopathies: classification and clinical update on neurodegenerative diseases associated with microtubule-associated protein tau. *Intern Med J*. 2006;36(10):652-660.

5. Prusiner SB. Cell biology: a unifying role for prions in neurodegenerative diseases. *Science*. 2012;336(6088):1511-1513.

6. Goedert M. Alzheimer's and Parkinson's diseases: the prion concept in relation to assembled Aβ, tau, and α-synuclein. *Science*. 2015;349(6248):1255555.

7. Grundke-Iqbal I, Iqbal K, Tung YC, Quinlan M, Wisniewski HM, Binder LI. Abnormal phosphorylation of the microtubule-associated protein tau (tau) in Alzheimer cytoskeletal pathology. *Proc Natl Acad Sci U S A*. 1986;83(13):4913-4917.

8. Kosik KS, Joachim CL, Selkoe DJ. Microtubule-associated protein tau (tau) is a major antigenic component of paired helical filaments in Alzheimer disease. *Proc Natl Acad Sci U S A*. 1986;83(11):4044-4048.

9. Wood JG, Mirra SS, Pollock NJ, Binder LI. Neurofibrillary tangles of Alzheimer disease share antigenic determinants with the axonal microtubule-associated protein tau (tau). *Proc Natl Acad Sci U S A*. 1986;83(11):4040-4043.

10. Goedert M, Spillantini MG, Potier MC, Ulrich J, Crowther RA. Cloning and sequencing of the cDNA encoding an isoform of microtubule-associated protein tau containing four tandem repeats: differential expression of tau protein mRNAs in human brain. *EMBO J*. 1989;8(2):393-399.

11. Goedert M, Spillantini MG, Cairns NJ, Crowther RA. Tau proteins of Alzheimer paired helical filaments: abnormal phosphorylation of all six brain isoforms. *Neuron*. 1992;8(1):159-168.

12. Götz J, Probst A, Spillantini MG, et al. Somatodendritic localization and hyperphosphorylation of tau protein in transgenic mice expressing the longest human brain tau isoform. *EMBO J*. 1995;14(7):1304-1313.

13. Probst A, Götz J, Wiederhold KH, et al. Axonopathy and amyotrophy in mice transgenic for human four-repeat tau protein. *Acta Neuropathol*. 2000;99(5):469-481.

14. Spittaels K, Van den Haute C, Van Dorpe J, et al. Prominent axonopathy in the brain and spinal cord of transgenic mice overexpressing four-repeat human tau protein. *Am J Pathol*. 1999;155(6):2153-2165.

15. Ishihara T, Hong M, Zhang B, et al. Age-dependent emergence and progression of a tauopathy in transgenic mice overexpressing the shortest human tau isoform. *Neuron*. 1999;24(3):751-762.

16. Brion JP, Tremp G, Octave JN. Transgenic expression of the shortest human tau affects its compartmentalization and its phosphorylation as in the pretangle stage of Alzheimer's disease. *Am J Pathol*. 1999;154(1):255-270.

17. Forman MS, Lal D, Zhang B, et al. Transgenic mouse model of tau pathology in astrocytes leading to nervous system degeneration. *J Neurosci*. 2005;25(14):3539-3550.

18. Andorfer C, Kress Y, Espinoza M, et al. Hyperphosphorylation and aggregation of tau in mice expressing normal human tau isoforms. *J Neurochem*. 2003;86(3):582-590.

19. Duff K, Knight H, Refolo LM, et al. Characterization of pathology in transgenic mice over-expressing human genomic and cDNA tau transgenes. *Neurobiol Dis*. 2000;7(2):87-98.

20. van Swieten J, Spillantini MG. Hereditary frontotemporal dementia caused by *Tau* gene mutations. *Brain Pathol*. 2007;17(1):63-73.

21. Frank S, Clavaguera F, Tolnay M. Tauopathy models and human neuropathology: similarities and differences. *Acta Neuropathol*. 2008;115(1):39-53.

22. Dujardin S, Colin M, Buée L. Invited review: animal models of tauopathies and their implications for research/translation into the clinic. *Neuropathol Appl Neurobiol*. 2015;41(1):59-80.

23. Yoshiyama Y, Higuchi M, Zhang B, et al. Synapse loss and microglial activation precede tangles in a P301S tauopathy mouse model [published correction appears in *Neuron*. 2007;54(2):343-344]. *Neuron*. 2007;53(3):337-351.

24. Holmes BB, Furman JL, Mahan TE, et al. Proteopathic tau seeding predicts tauopathy in vivo. *Proc Natl Acad Sci U S A*. 2014;111(41):E4376-E4385.

25. Kaufman SK, Thomas TL, Del Tredici K, Braak H, Diamond MI. Characterization of tau prion seeding activity and strains from formaldehyde-fixed tissue. *Acta Neuropathol Commun*. 2017;5(1):41.

26. Allen B, Ingram E, Takao M, et al. Abundant tau filaments and nonapoptotic neurodegeneration in transgenic mice expressing human P301S tau protein. *J Neurosci*. 2002;22(21):9340-9351.

27. Woerman AL, Stöhr J, Aoyagi A, et al. Propagation of prions causing synucleinopathies in cultured cells. *Proc Natl Acad Sci U S A*. 2015;112(35):E4949-E4958.

28. Committee for the Update of the Guide for the Care and Use of Laboratory Animals, Institute for Laboratory Animal Research, Division of Earth and Life Sciences, National Research Council of the National Academies. *Guide for the Care and Use of Laboratory Animals*. 8th ed. Washington, DC: National Academies Press; 2011.

29. C57BL/6J (B6/J) Mice [Internet]. The Jackson Laboratory. https://www.jax.org/strain/000664. Accessed August 30, 2017.

30. Safar J, Wille H, Itri V, et al. Eight prion strains have PrP^{Sc} molecules with different conformations. *Nat Med*. 1998;4(10):1157-1165.

31. Woerman AL, Aoyagi A, Patel S, et al. Tau prions from Alzheimer's disease and chronic traumatic encephalopathy patients propagate in cultured cells. *Proc Natl Acad Sci U S A*. 2016;113(50):E8187-E8196.

32. Sanders DW, Kaufman SK, DeVos SL, et al. Distinct tau prion strains propagate in cells and mice and define different tauopathies. *Neuron*. 2014;82(6):1271-1288.

33. Falcon B, Cavallini A, Angers R, et al. Conformation determines the seeding potencies of native and recombinant tau aggregates. *J Biol Chem*. 2015;290(2):1049-1065.

34. Giasson BI, Duda JE, Quinn SM, Zhang B, Trojanowski JQ, Lee VM. Neuronal α-synucleinopathy with severe movement disorder in mice expressing A53T human α-synuclein. *Neuron*. 2002;34(4):521-533.

35. Yoshiyama Y, Uryu K, Higuchi M, et al. Enhanced neurofibrillary tangle formation, cerebral atrophy, and cognitive deficits induced by repetitive mild brain injury in a transgenic tauopathy mouse model. *J Neurotrauma*. 2005;22(10):1134-1141.

36. Watts JC, Giles K, Oehler A, et al. Transmission of multiple system atrophy prions to transgenic mice. *Proc Natl Acad Sci U S A*. 2013;110(48):19555-19560.

37. Brunden KR, Zhang B, Carroll J, et al. Epothilone D improves microtubule density, axonal integrity, and cognition in a transgenic mouse model of tauopathy. *J Neurosci*. 2010;30(41):13861-13866.

38. Zhang B, Carroll J, Trojanowski JQ, et al. The microtubule-stabilizing agent, epothilone D, reduces axonal dysfunction, neurotoxicity, cognitive deficits, and Alzheimer-like pathology in an interventional study with aged tau transgenic mice. *J Neurosci*. 2012;32(11):3601-3611.

39. Yanamandra K, Kfoury N, Jiang H, et al. Anti-tau antibodies that block tau aggregate seeding in vitro markedly decrease pathology and improve cognition in vivo. *Neuron*. 2013;80(2):402-414.

40. Zhang Z, Obianyo O, Dall E, et al. Inhibition of δ-secretase improves cognitive functions in mouse models of Alzheimer's disease. *Nat Commun*. 2017;8:14740.

41. Wisely EV, Xiang YK, Oddo S. Genetic suppression of β2-adrenergic receptors ameliorates tau pathology in a mouse model of tauopathies. *Hum Mol Genet*. 2014;23(15):4024-4034.

42. Wagner J, Krauss S, Shi S, et al. Reducing tau aggregates with anle138b delays disease progression in a mouse model of tauopathies. *Acta Neuropathol*. 2015;130(5):619-631.

43. Stack C, Jainuddin S, Elipenahli C, et al. Methylene blue upregulates Nrf2/ARE genes and prevents tau-related neurotoxicity. *Hum Mol Genet*. 2014;23(14):3716-3732.

44. Sankaranarayanan S, Barten DM, Vana L, et al. Passive immunization with phospho-tau antibodies reduces tau pathology and functional deficits in two distinct mouse tauopathy models. *PLoS One*. 2015;10(5):e0125614.

45. Richter M, Mewes A, Fritsch M, Krügel U, Hoffmann R, Singer D. Doubly phosphorylated peptide vaccines to protect transgenic P301S mice against Alzheimer's disease like tau aggregation. *Vaccines (Basel)*. 2014;2(3):601-623.

46. Ohia-Nwoko O, Montazari S, Lau YS, Eriksen JL. Long-term treadmill exercise attenuates tau pathology in P301S tau transgenic mice. *Mol Neurodegener*. 2014;9:54.

47. Min SW, Chen X, Tracy TE, et al. Critical role of acetylation in tau-mediated neurodegeneration and cognitive deficits. *Nat Med*. 2015;21(10):1154-1162.

48. Makani V, Zhang B, Han H, et al. Evaluation of the brain-penetrant microtubule-stabilizing agent, dictyostatin, in the PS19 tau transgenic mouse model of tauopathy. *Acta Neuropathol Commun*. 2016;4(1):106.

49. Elipenahli C, Stack C, Jainuddin S, et al. Behavioral improvement after chronic administration of coenzyme Q10 in P301S transgenic mice. *J Alzheimers Dis*. 2012;28(1):173-182.

50. Dumont M, Stack C, Elipenahli C, et al. Bezafibrate administration improves behavioral deficits and tau pathology in P301S mice. *Hum Mol Genet*. 2012;21(23):5091-5105.

51. Caccamo A, Magrì A, Medina DX, et al. mTOR regulates tau phosphorylation and degradation: implications for Alzheimer's disease and other tauopathies. *Aging Cell*. 2013;12(3):370-380.

52. Asai H, Ikezu S, Tsunoda S, et al. Depletion of microglia and inhibition of exosome synthesis halt tau propagation. *Nat Neurosci*. 2015;18(11):1584-1593.

53. Carlson GA, Goodman PA, Lovett M, et al. Genetics and polymorphism of the mouse prion gene complex: control of scrapie incubation time. *Mol Cell Biol*. 1988;8(12):5528-5540.

54. Dickinson AG. Host-pathogen interactions in scrapie. *Genetics*. 1975;79(suppl):387-395.

55. Kingsbury DT, Kasper KC, Stites DP, Watson JD, Hogan RN, Prusiner SB. Genetic control of scrapie and Creutzfeldt-Jakob disease in mice. *J Immunol*. 1983;131(1):491-496.

56. Stephenson DA, Chiotti K, Ebeling C, et al. Quantitative trait loci affecting prion incubation time in mice. *Genomics*. 2000;69(1):47-53.

57. Lloyd SE, Onwuazor ON, Beck JA, et al. Identification of multiple quantitative trait loci linked to prion disease incubation period in mice. *Proc Natl Acad Sci U S A*. 2001;98(11):6279-6283.

58. Götz J, Ittner LM. Animal models of Alzheimer's disease and frontotemporal dementia. *Nat Rev Neurosci*. 2008;9(7):532-544.

59. Gordon JW, Chesa PG, Nishimura H, et al. Regulation of Thy-1 gene expression in transgenic mice. *Cell*. 1987;50(3):445-452.

60. Caroni P. Overexpression of growth-associated proteins in the neurons of adult transgenic mice. *J Neurosci Methods*. 1997;71(1):3-9.

61. Scott M, Foster D, Mirenda C, et al. Transgenic mice expressing hamster prion protein produce species-specific scrapie infectivity and amyloid plaques. *Cell*. 1989;59(5):847-857.